Electronic Spectroscopy and Ultrafast Energy Relaxation Pathways in the Lowest Rydberg States of Trimethylamine

Job D. Cardoza, Fedor M. Rudakov, and Peter M. Weber*

Department of Chemistry, Brown University, Providence, Rhode Island 02912

Received: May 9, 2008; Revised Manuscript Received: August 18, 2008

Resonance-enhanced multiphoton ionization photoelectron spectroscopy has been applied to study the electronic spectroscopy and relaxation pathways among the 3p and 3s Rydberg states of trimethylamine. The experiments used femtosecond and picosecond duration laser pulses at wavelengths of 416, 266, and 208 nm and employed two-photon and three-photon ionization schemes. The binding energy of the 3s Rydberg state was found to be 3.087 ± 0.005 eV. The degenerate $3p_{x,y}$ states have binding energies of 2.251 ± 0.005 eV, and $3p_z$ is at 2.204 ± 0.005 eV. Using picosecond and femtosecond time-resolved experiments we spectrally and temporally resolved an intricate sequence of energy relaxation pathways leading from the 3p states to the 3s state. With excitation at 5.96 eV, trimethylamine is found to decay from the $3p_z$ state to $3p_{x,y}$ in 539 fs. The decay to 3s from all the 3p states takes place with a 2.9 ps time constant. On these time scales, trimethylamine does not fragment at the given internal energies, which range from 0.42 to 1.54 eV depending on the excitation wavelength and electronic state.

1. Introduction

In spite of a long history of research,[1] the high-lying electronic states and electronic relaxation processes in polyatomic molecules with multiple degrees of freedom remain remarkably uncharted. Even when cooled in free jet expansions or molecular beams, the spectra often remain unresolved because of broad Franck−Condon envelopes that arise from dramatically changing potential energy surfaces upon electronic excitation. Moreover, homogeneous broadening of individual levels results from the short lifetimes that are typical for high-lying electronic states. Finally, electronic transitions associated with the dense manifold of highly excited states often overlap to prevent a clear look at individual electronic states.

All these factors play a role in the spectra of the aliphatic amines, where even the lowest excited electronic states are of Rydberg character.[2] Starting with the well-resolved vibronic spectra of ammonia,[3−8] the spectra of the primary, secondary, and tertiary aliphatic amines become increasingly congested.[2] In the tertiary amines, only broad bands without distinct features are seen in absorption. This is unfortunate because, in general, the optical properties of molecules are important as benchmarks for theoretical studies. The aliphatic amines are especially important because they act as chromophores in peptides and other important biological systems such as neurotransmitters. Moreover, amines are present in many energetic materials and also appear as impurities and decomposition products of those substances.

Methylated amines have frequently been used as root compounds for the larger set of aliphatic amines. They all feature pyramidal ground electronic states and planar Rydberg excited states, and they have internal rotations associated with the methyl groups.[2] The smallest tertiary amine, trimethylamine (TMA), $N(CH_3)_3$, has been used as a prototype to explore the spectroscopy and photochemistry of this class of compounds.[9−11] Among the amines, the tertiary amines have the lowest ionization energies,[12] causing the Rydberg series to start at a relatively low energy, about 4.5 eV. At excitation wavelengths below 220 nm, TMA has a very low fluorescence quantum yield,[13] and following excitation at 193 nm it converts to the ground state surface and dissociates a methyl radical to form the $N(CH_3)_2$ product.[14,15]

The three methyl rotor groups provide trimethylamine with a set of dense, low-frequency vibrations that prevent observation of any vibrationally resolved absorption or fluorescence spectra. The absorption spectrum features a broad band between 250 and 220 nm that is assigned to the $3s \leftarrow n_N$ ($\tilde{A}\ ^1A_2'' \leftarrow \tilde{X}\ ^1A_1$) transition.[2,9] Halpern et al. used very high quality absorption spectra and a second-derivative analysis technique to identify the vibrational progressions within this $\tilde{A} \leftarrow \tilde{X}$ transition.[16] Their work pegs the origin transition at 266 nm. At the high-energy side, the 3s band overlaps with the absorption to the 3p levels, all of which coalesce in a featureless, broad band with a maximum at 199 nm.[2] Because of this spectral overlap, explorations of the electronic relaxation phenomena between the 3p states and from 3p to 3s have to date not been possible.

The unresolved Rydberg transitions in trimethylamine have also been explored by Taylor et al.,[17] who used multiphoton ionization coupled with mass-resolved photoion detection to obtain mass-resolved excitation spectra (MRES). As had been observed in absorption,[2] the MRES exhibits no clear vibrational structure in trimethylamine, and the most prominent feature, a peak near 44 000 cm^{-1} excitation energy, is difficult to assign due to the overlap of the 3s and 3p Rydberg states in this region.[9]

In our recent work we demonstrated that crisp electronic spectra, showing clearly even close-lying electronic states of highly vibrationally excited molecules, can be obtained by choosing electronic transitions that do not couple to vibrational degrees of freedom.[18,19] As we showed specifically on trimethylamine, ionization from a Rydberg state to the associated state of the ion satisfies this condition.[20] We applied this idea to develop a molecular shape fingerprint spectroscopy,[21] which has found useful applications in, among other areas, identification of the charge center in a bifunctional molecule,[22] determi-

* To whom correspondence should be addressed. E-mail: Peter_Weber@brown.edu.

10.1021/jp8041236 CCC: $40.75
Published on Web 10/04/2008

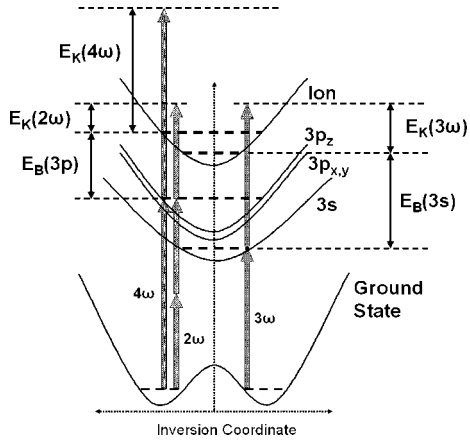

Figure 1. Ionization schemes employed in the experiments. The 3p Rydberg states are accessed in one- and two-photon absorption processes using the fourth and second harmonics of the titanium−sapphire laser, respectively. Subsequent ionization requires a single fourth, third, or second harmonic photon. The 3s Rydberg state is accessed directly with a third-harmonic photon and ionized using an additional photon of the same color. Time-dependent measurements involve either fourth-harmonic excitation and second-harmonic ionization or second-harmonic excitation and third-harmonic ionization. Internally converted products in 3s can only be ionized with third-harmonic photons.

nation of chemical reaction pathways,[23] and observation of the conformeric dynamics in hot hydrocarbons.[19] In the present paper we apply this technique to investigate the electronic spectroscopy and relaxation dynamics of the low-lying Rydberg states of trimethylamine, a compound that is notorious for its unresolved electronic absorption spectrum.

In our experiment (Figure 1) we access the 3p Rydberg states by either single-photon or two-photon excitation. For the one-photon excitation we use the fourth harmonic of the titanium-sapphire laser (4ω), while for the two-photon excitation we use the second harmonic (2ω). From the Rydberg states, the molecules are ionized in a single-photon process, producing photoelectrons that are analyzed for their kinetic energy E_K. By subtracting this electron kinetic energy from the energy of the ionizing photon we obtain the spectra of the Rydberg state binding energies, E_B, that are shown throughout this paper.

Photoionization out of Rydberg states has two inherent advantages, which both result from the fact that the potential energy surfaces of Rydberg states are very similar to those of the corresponding ions. First, the transition from a Rydberg state to an ion is associated with $\Delta v = 0$ selection rules,[24,25] implying that the vibrational quantum states do not change. Second, the vibrational frequencies of the Rydberg states are almost identical to those of the ion. As a result, all vibrational transitions bunch up at the same energy within the electronic band, giving rise to sharp spectral lines even when much internal energy is distributed among the vibrations.[18,26−28] As we discuss below, even the presence of the highly excited methyl rotors in trimethylamine does not wash out the spectra.[29,30]

The lifetimes of the 3p states of trimethylamine are short but not so short that spectral separation of the 3p states is impossible. In past work, photoionization photoelectron spectroscopy experiments have been performed on trimethylamine using nanosecond laser pulses.[10,31] That time scale is poorly matched to the molecular dynamics because the molecules initially prepared in 3p convert to 3s within the duration of the nanosecond pulse, so that ionization always proceeds out of the latter. Our experiments were performed with pulses of femtosecond and picosecond duration. The femtosecond time-resolved experiments allowed us to time resolve the dynamical processes, while the picosecond experiments better resolved the underlying electronic levels. This combination of the spectrally and temporally resolved experiments uncovered an intricate web of sequential and parallel decay processes that is described in this paper.

2. Experimental Section

The lasers and photoelectron spectrometer have been described in detail previously.[32,33] For the experiments discussed here, two separate laser systems were used. Both use a titanium−sapphire oscillator laser and an Nd:YLF-pumped titanium−sapphire regenerative amplifier. The first amplifier, running at a repetition rate of 50 kHz, delivers pulses with about 100 fs duration at wavelengths near 800 nm. The second laser system, operating at 5 kHz, was set to provide 2 ps pulses with a correspondingly narrow bandwidth of 2 nm at wavelengths near 800 nm. With an interchange of optics, the 5 kHz amplifier was also able to generate broad bandwidth 50 fs pulses near 800 nm, which we used in some of the femtosecond time-resolved experiments. The outputs of the laser systems were upconverted to second, third, and fourth harmonics using BBO crystals. The tuning range of the Ti:Sapphire lasers allowed us to set the wavelengths of the second harmonic between 390 and 420 nm, the third harmonic between 260 and 280 nm, and the fourth harmonic between 207 and 210 nm. The pulse energies of these higher harmonics are typically 0.8, 0.3, and 0.2 μJ, respectively, for the 50 kHz laser. The pulse energy of the 5 kHz laser at the second harmonic wavelength was 16 μJ, while at the third and fourth harmonic wavelengths the pulse energies were 2.4 and 0.6 μJ, respectively. Each of the higher harmonic beams was mildly focused onto a molecular beam in the photoelectron spectrometer using a 200 mm UV-grade fused silica lens. The second, third, and fourth harmonic intensities at the interaction region are estimated to be 1.4×10^{12}, 2.7×10^{11}, and 1.1×10^{11} W/cm^2, respectively, for the 50 kHz laser. For the 5 kHz laser in picosecond mode, the second, third, and fourth harmonic intensities at the interaction region are estimated to be 1.6×10^{12}, 1.3×10^{11}, and 1.7×10^{10} W/cm^2, respectively. In femtosecond mode, the corresponding intensities are 3.1×10^{13}, 2.7×10^{12}, and 3.4×10^{11} W/cm^2.

The molecular beam is generated by expansion of trimethylamine vapor, seeded in a helium carrier gas at 1 bar, through a nozzle orifice with a 100 μm diameter and skimmer with a 150 μm diameter. The beam is oriented normally to the laser beam propagation axis. Anhydrous trimethylamine was purchased from Sigma-Aldrich and used without further purification. Since TMA at room temperature is a gas, it was cooled to −60 °C for seeding in the carrier gas for all spectra except the one in Figure 3a, which was taken at a temperature of −30 °C to improve the signal. Certainly at the lower temperature the vapor pressure of TMA is small enough to avoid formation of clusters in the jet expansion.

3. Results and Discussion

3.1. Spectroscopy. Rydberg state binding energy spectra recorded using resonant two-photon ionization are shown in Figure 2a, showing the spectrum for ionization with two femtosecond laser photons at 209 nm. The spectrum features two clearly resolved peaks: the one around 3.1 eV is from the 3s level, while the peak near 2.2 eV results from ionization via 3p. The energy of the 209 nm photons, 5.93 eV, is quite large and results in the ejection of fast electrons for which the energy is difficult to measure (see Figure 1). Therefore, the spectra have

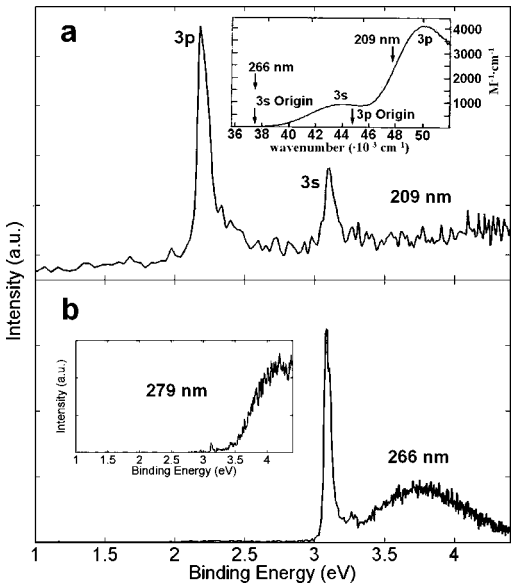

Figure 2. (a) One-photon resonant two-photon ionization photoelectron spectrum at 209 nm, taken using femtosecond pulses from the 50 kHz regenerative amplifier. The ultraviolet absorption spectrum, adapted from ref 16 in the region of the 3s and 3p Rydberg states, is shown in the inset. Arrows identify the energies of the 3s and 3p states as determined here as well as the energies of the 209 and 266 nm photons. (b) One-photon resonant two-photon ionization photoelectron spectrum at 266 nm, taken with the 50 kHz regenerative amplifier. For comparison, the inset shows the two-photon ionization photoelectron spectrum at 279 nm.

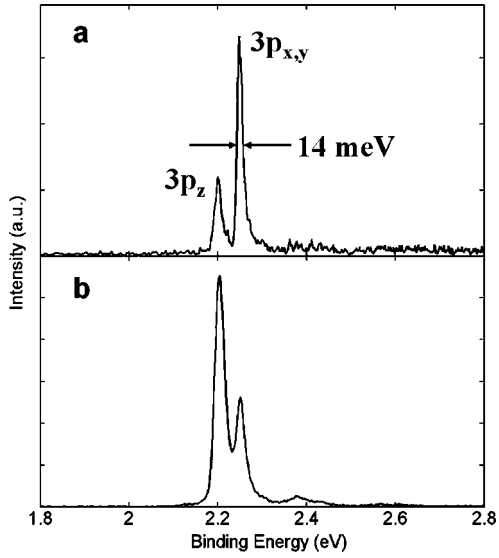

Figure 3. (a) Two-photon resonant three-photon ionization photoelectron spectrum at 416 nm, taken with picosecond duration pulses from a 5 kHz regenerative amplifier to optimize the energy resolution. (b) The one-photon resonant, two-color photoelectron spectrum. In this spectrum, a fourth harmonic femtosecond laser pulse at 208 nm was used for excitation and a second harmonic femtosecond laser pulse at 416 nm was used for ionization, both of which were generated using a 50 kHz regenerative amplifier. The spectrum was taken where the two pulses are temporally superimposed.

rather poor resolution, insufficient to resolve the individual 3p levels. Even using a narrow bandwidth picosecond laser, the 3p levels are still unresolved (data not shown), indicating the resolution limit is approximately 50 meV or more at this photon energy. Excitation at 209 nm leads almost exclusively to 3p.[9] Ionization out of 3s is nonetheless observed because the far UV laser pulses are temporally broadened by dispersive optical elements. As we describe below, the internal conversion from 3p to 3s is rapid and effectively competes with ionization within the laser pulse.

Panel b of Figure 2 shows the binding energy spectrum obtained with femtosecond laser pulses at 266 nm. According to Halpern et al.,[16] whose absorption spectrum is reproduced as an inset in Figure 2a, this wavelength is just at the origin transition to the 3s band at the very onset of the Franck−Condon envelope. Even though the photoionization efficiency at 266 nm is rather poor, a long data acquisition time allowed us to obtain a good quality spectrum. It shows a single sharp peak, reflecting ionization out of the 3s level with a binding energy of 3.087 ± 0.005 eV. As we previously reported,[20] using the energy of the origin transition to the 3s level by Halpern et al. of 4.656 eV and our measured binding energy of 3.087 eV, this implies an adiabatic ionization energy (IE) of 7.743 eV. This value is in good agreement with the one by Aue et al., who report an adiabatic IE of 7.76 eV.[34]

The two-photon ionization spectrum Figure 2b also shows a broad, unresolved band stretching from 3.4 to 4.3 eV in the binding energy spectrum. Using our apparatus in mass spectrometry mode, we observed that van der Waals clusters of TMA can be easily generated when the sample bath temperature is −50 °C or higher. Those clusters, for which we observed multimers containing up to 23 TMA molecules, give rise to a broad feature similar to the one of Figure 2b. However, at the sample temperature used here, −60 °C, the mass spectra show no sizable signal from clusters. The broad band must therefore come from the monomer. Since no other electronic states have been found in this range,[35,36] it must arise from a competing photoionization pathway that does not take advantage of the very weak 3s resonance enhancement. Without resonance, the photoelectron spectrum is expected to show a vertical ionization feature reflecting many unresolved transitions to vibrational states of the ion. The vertical IE of TMA given by Kimura et al.[12] is 8.44 eV, which is 0.70 eV above the adiabatic IE determined above. This energy increment is mirrored nicely as the difference in energy between the broad band and the sharp Rydberg peak of Figure 2b. We conclude that the broad feature is likely from the nonresonant ionization path leading to high-lying vibrations of the ion. This path competes effectively with the resonant pathway because the Franck−Condon factors from the ground state to the origin level of the 3s Rydberg state are so weak. The inset in Figure 2b shows the two-photon ionization spectrum taken at a longer wavelength, 279 nm. The photon energy is now below that of the origin transition to 3s. As a result, only the nonresonant pathway remains for ionization, and we observe only the unresolved broad part of the spectrum.

Photoionization out of the Rydberg levels using a longer laser wavelength leads to ejection of slower electrons, of which the energy can be measured with higher resolution. Figure 3 shows two such spectra. In Figure 3a photoionization is achieved with three photons at 416 nm using the 3p level as a two-photon resonance. To optimize the energy resolution of this spectrum, a 2 ps pulse duration and a narrow bandwidth were used. Since the pulse duration is long compared to the 3p lifetimes, the intensities of those peaks do not reflect their relative excitation cross sections.

Figure 3b is obtained in a two-color two-photon ionization scheme using a 208 nm photon to prepare the molecule in 3p and a 416 nm photon to probe the levels. In order to minimize any decay of the levels between the two photons, femtosecond laser pulses were used for this spectrum and the time delay between the excitation and ionization pulses was set to zero.

TABLE 1: Vertical Ionization Energy (IE) and Vertical Excitation Energies to Rydberg States As Observed in Absorption and Photoionization Experiments (See References) and Calculated Using a DFT-B3LYP with a 6-311+G Basis Set[a]**

		3s		$3p_{x,y}$		$3p_z$	
	vertical IE	Vertical excitation energy	Intensity	Vertical excitation energy	Intensity	Vertical excitation energy	Intensity
experiment	8.44 eV[b]	5.460 eV[c] (227.1 nm)	0.018[c]			6.229 eV[d] (199.1 nm)	0.13[d]
calculation	8.678 eV	5.476 eV (226.4 nm)	0.022	6.161 eV (201.3 nm)	0.0066	6.307 eV (196.6 nm)	0.102

[a] For the calculation, the ground-state molecular structure from ref 38 was used: the molecule is pyramidal with a C−N bond length of 1.472 Å, a C−H bond length of 1.096 Å, and a C−N−C bond angle of 108.7°. The methyl groups were oriented such that three of the C−H bonds on different carbon atoms are opposite to the nonbonding orbital on nitrogen and aligned almost parallel the C_3 axis. [b] From photoelectron spectra, ref 12. [c] From absorption spectra, ref 16. [d] From absorption spectra, ref 2.

While the spectral resolution is not as good as that of Figure 3a, the spectrum reflects more accurately the relative intensities upon excitation to the 3p levels, which is > 9:1 as described in section 3.2.2 below. Both spectra of Figure 3 show nicely resolved peaks reflecting two Rydberg levels at $E_B = 2.204 \pm 0.005$ and 2.251 ± 0.005 eV. Neither spectrum shows ionization out of 3s because the energy of the 416 nm photons is too low for ionization.

3.1.1. Assignments. Assignment of the 3p levels can be based on analogy with ammonia and consideration of the relative peak intensities. In ammonia, the lower binding energy peak was assigned to $3p_z$.[4,6,7] In analogy, we should assign the level with $E_B = 2.204$ eV to the $3p_z$ state.

The ionization intensities out of the $3p_z$ and $3p_{x,y}$ Rydberg states are most likely quite similar. We can therefore assume that the observed relative peak intensities reflect probabilities of exciting the initial 3p states. A qualitative consideration of the orbital geometries and their overlap suggests that the $3p_z \leftarrow$ n transition should have a higher intensity than the degenerate $3p_{x,y} \leftarrow$ n transition. However, early ab initio calculations of Avouris and Rossi are in disagreement with this conjecture.[37] Since that work was done, calculations with larger basis sets have become possible. We performed a DFT calculation of trimethylamine at the B3LYP level with a 6-311+G** basis set. To calculate vertical ionization and excitation energies we used the structure from microwave measurements by Lide and Mann[38] because it yielded the best agreement between the computed and the experimentally measured electronic energies. The computed vertical ionization energies and excitation energies as well as the oscillator strengths are compared with experimental data from the literature in Table 1. The intensity calculated for absorption to the $3p_z$ level is much higher than that to the $3p_{x,y}$ level, as expected from the qualitative arguments. We therefore assign the more intense peak in our two-photon ionization photoelectron spectrum (Figure 3b) with $E_B = 2.204$ eV to $3p_z$. The peak with $E_B = 2.251$ eV belongs to $3p_{x,y}$. This assignment agrees with the one made earlier using the analogy to ammonia.

The Franck−Condon envelopes for absorption to the Rydberg states and ion state are nearly identical. It is therefore possible to extract the electron binding energies of the Rydberg states by subtracting the computed vertical excitation energies to the Rydberg states from the computed vertical ionization energy. The electron binding energies of the Rydberg states calculated in this way, Table 2, are in reasonable agreement with the experimental results. All calculated values are too high by 0.115−0.266 eV. The experimental value for the separation between the different 3p levels, 0.047 ± 0.002 eV, can be determined quite accurately because systematic errors cancel out. The calculated value, 0.156 eV, is again too high by about 0.1 eV or 2.3 kcal/mol. Given the high electronic energy of the Rydberg states, this level of accuracy is reasonable given the scale of the calculation.

TABLE 2: Electron Binding Energies for the Low-n Rydberg States of TMA[a]

	$E_B(3s)$, eV	$E_B(3p_{x,y})$, eV	$E_B(3p_z)$, eV	ΔE $(3p_{x,y} - 3p_z)$, eV
experiment	3.087	2.251	2.204	0.047
calculation	3.202	2.517	2.371	0.146

[a] The experimental values were obtained by photoionization from the Rydberg states, while the computed values were derived using the data of Table 1, assuming constancy of the Franck−Condon envelopes for excitation from the ground state to the Rydberg and ion states.

In a recent publication, Taylor et al. suggested that trimethylamine has two 3s Rydberg states, a bound one at 5.535 eV and a dissociative state at 5.852 eV.[17] The authors base their reasoning on CAS-MP2 calculations with a double-ζ valence plus polarization (DZP) basis set augmented by 3s or 3p Rydberg orbitals on the nitrogen and carbon atoms and on a mass-resolved excitation spectrum. The occurrence of two 3s Rydberg states was explained as arising from different charge distributions in the ion core. Our electronically resolved spectra show no signature of such states. It might be argued (implausibly) that the excitation wavelengths of our lasers are such that we just miss the postulated dissociative Rydberg states. As part of our study of the relaxation processes within the Rydberg manifold of trimethylamine described below, we aim to investigate if any dissociative Rydberg states might play a role in the molecule's energy conversion processes.

3.1.2. Spectral Resolution. The photoionization spectra out of trimethylamine's Rydberg states show an excellent spectral resolution, even though a significant amount of energy is inserted into the molecule during the excitation process. The spectrum of Figure 3a, taken with the picosecond laser pulses, features a full width at half-maximum (fwhm) of 14 meV, which is at the resolution limit of the electron spectrometer for $E_K = 0.8$ eV electrons. The spectrum of Figure 2b has a fwhm of 47 meV as given by the bandwidth of the femtosecond laser pulses.

The excitation at 208 nm (5.961 eV) deposits 0.422 eV of energy into the vibrational manifold of the $3p_z$ level, which is at an adiabatic energy of 7.743−2.204 eV = 5.539 eV. Assuming equipartitioning of that energy among all vibrational modes,[39] the effective temperature is 660 K. Once the molecule converts to 3s, the internal vibrational energy increases to 1.313 eV and the temperature increases to 1170 K. We note that the total energy distributed among vibrations is far above the barrier to methyl rotation, which is 0.157 eV.[40] One expects that a large number of vibrational and internal rotation states are excited in the Rydberg states. Even so, the vibronic transitions from the Rydberg levels to the ions all bunch up at the same energy because the vibrational quantum numbers are conserved and the vibrational frequencies remain unchanged. The combined spectral broadening arising from all these vibrational motions and the rotations of the methyl groups is less than the instrumental resolution of 14 meV. It is evident that photoion-

ization is an excellent method for observing the purely electronic spectra of Rydberg states. In the following section we will apply this insight to investigate the electronic relaxation between the Rydberg levels of TMA.

3.2. Dynamics. To probe the ultrafast electronic relaxation dynamics among the Rydberg states, we employed two separate time-resolved pump−probe schemes. In the first scheme, the 3p states are prepared by two-photon excitation using laser pulses around 400 nm (second harmonic). The time-delayed third harmonic pulses at 266 nm are used to ionize the molecules. Since upconversion crystals pose no wavelength limitation for generation of the second and third harmonics, we performed experiments at two wavelengths. The advantage of this three-photon scheme is that the probe photons are sufficiently energetic to ionize from any of the Rydberg states. The drawback is that the ejected electrons are fast, so that the spectral resolution of the photoelectron spectrometer is inadequate to resolve the individual 3p levels. In addition, it turned out to be difficult to attain a good signal-to-noise ratio because for small second harmonic pulse energies the signal was low and for high pulse energies the one-color signal would dominate the spectrum.

In the second scheme, we prepared the 3p levels directly using one-photon excitation. Upconversion crystals to the fourth harmonic limit this scheme to only a small wavelength range. We used 207.8 nm for excitation and the second harmonic 415.6 nm for ionization. For ionization out of 3p, this yields slow electrons for which the energy can be well measured. As a result, this two-photon pump−probe scheme allows us to spectrally separate the nondegenerate 3p states. On the other hand, the ionization photon energy is insufficient to ionize out of 3s, so that this experiment cannot probe the participation of the 3s level in the electronic relaxation dynamics. We therefore use the three-photon scheme to establish the 3p → 3s pathway for electronic relaxation but the two-photon scheme to derive the time constants.

3.2.1. Three-Photon Experiments. Two-color, three-photon experiments have been performed using wavelengths of 418/279 and 400/266 nm. The longer wavelength photons prepare the 3p states, and the dynamics is probed using time-delayed pulses at 279 and 266 nm, respectively. Figure 4a shows a contour plot with the time-dependent photoelectron spectrum obtained at 400/266 nm, taken with the 5 kHz laser. Even though the spectral resolution is low, the 3p states near $E_B = 2.2$ eV are well separated from the 3s state at 3.1 eV. The 3p peak shows a time-dependent shift at the early delay times, foreshadowing the dynamics within 3p that we will see more clearly below. To fit the data of Figure 4a, we summed up the intensity over the entire 3p band as well as that of the 3s band. Figure 4b shows the fits obtained by assuming a first-order exponential decay of the 3p states and rise of the 3s signal. Both the decay of 3p and the rise of 3s are well represented by a single time constant, 2.0 ps, suggesting that the decay of 3p leads directly to 3s. (A better determination of the lifetime results from the two-photon experiments discussed below.) Because the decay of 3p and rise of 3s are with the same time constant and there is no other signal with a rise time that reflects the decay of 3p, we postulate that no electronic states other than 3p and 3s are prepared in the initial excitation or participate in the electronic relaxation scheme.

However, the contour plot of Figure 4a does show additional signal. At zero delay time there is a broad band, which is punctuated by several weak maxima. Since photoionization from Rydberg levels always results in well-resolved peaks, the origin

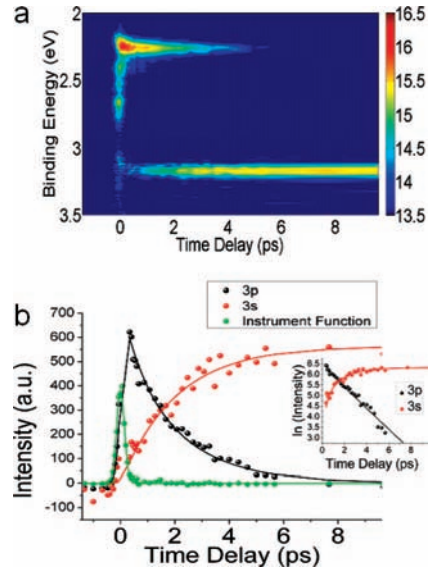

Figure 4. Time-dependent photoionization−photoelectron spectra of TMA upon excitation with two photons at 400 nm and ionization at 266 nm. (a) Time-dependent contour plot of the photoelectron spectra; the color represents the intensity on a logarithmic scale; the color bar gives the natural logarithm of the intensities in arbitrary units. The electron binding energy is plotted as the ordinate, arranged such that higher energy levels, i.e., levels with lower binding energy, are higher on the vertical axis. (b) Exponential fits for the time-dependent internal conversion of 3p into 3s using an instrument function that was obtained from the broad signal at time zero seen in panel a.

of the broad component of this signal must involve nonresonant ionization pathways or pathways via valence states. The narrow confinement of this signal to time zero suggests that it might be due to ionization in a three-photon sequence such as 400 nm → 266 nm → 400 nm. In this sequence, any time delay in either direction leads to a rapid loss of signal no matter how long-lived any intermediate state may be. This allows us to use this fast transient as an instrument function, as we have done in the analysis resulting in Figure 4b. Two small peaks that barely rise above the broad band are at apparent binding energies of 2.65 and 2.4 eV. If one corrects for the different photon energy of the ionization step, 400 nm instead of 266 nm, these peaks would correspond to binding energies of 1.09 and 0.84 eV, respectively. This would place them at $n = 4$, $\delta = 0.47$ and $n = 5$, $\delta = 0.98$, respectively, suggesting that they might arise from the 4p and 5s Rydberg states, respectively. (The 3p and 3s states have quantum defects of $\delta = 0.51$ and 0.90).

In previous experiments on *N*,*N*-dimethyl-2-propanamine we established a correlation between the decay from 3p to 3s and appearance of fragments in the mass spectrum.[29,30] Fragmentation proceeds in the ion as a result of the internal energy deposited in the molecule during the electronic relaxation. In trimethylamine, we found no mass signal with a time profile corresponding to the decay of the 3p Rydberg states. The dominant mass signal is due to the parent ion, and it shows only a step function like onset at time zero. When two 400 nm photons are used for excitation, there is a small fragment signal at mass 58 (loss of one hydrogen atom), amounting to only about 0.8% of the parent signal. At time zero it shows a spike, and after that it remains constant. The most plausible explanation for this feature is that it arises from the same process that gives rise to the broad structure found in the photoelectron spectrum at time zero (Figure 4a). During the process that gives rise to this ionization signal, some of the molecules are generated with an energy above the onset for dissociation of a C−H bond,

which has been determined to be 9.38 eV.[41] Those molecules can then fragment on their way to the mass spectrometer detector.

Further fragments at masses 42 and 44 are observed with even smaller intensities. Their time profile shows only a step function onset at time zero upon which they remain at a constant level. The constant signal at longer delay times, observed for all fragment peaks, can be explained as arising from a three-photon ionization with the 400 nm pulse followed by excitation of the ion by a 266 nm photon. From the photoelectron spectrum it is well known that trimethylamine cations have an absorption at 4.6 eV, stemming from excitation of a core electron to the HOMO.[12] This excitation deposits so much energy into the molecule that all observed fragmentation processes become possible.

To probe the dependence of the electronic relaxation dynamics on their vibrational energy content, we also performed measurements at pump/probe wavelengths of 418/279 nm. Within the uncertainties related to the rather poor signal-to-noise ratio of the three-photon pump−probe experiments, the decay time of 3p at longer wavelength equals that at the shorter one (we measured 2.1 ps).

3.2.2. Two-Photon Experiments. Experiments were performed using an excitation wavelength of 207.8 nm, which prepares the 3p levels at nearly the same energy as the two-photon excitation with the 418 nm laser. The ionization proceeds with a single second harmonic photon. Figure 5a presents the time-dependent spectrum with time displayed on the abscissa and binding energy as the ordinate. The binding energy is plotted on an inverted scale to remind the viewer that the smaller binding energy is higher above the ground state of the molecule. The time-dependent signal intensity is encoded by the color scales as given by the color bar. The scale is logarithmic, which offers a view of the signal over a wide dynamic range.

Since the photon energy, 2.99 eV, is insufficient to ionize out of 3s, the spectrum shows only ionization from 3p. The plots of Figure 5 therefore zoom in on the range from 2.1 to 2.4 eV. Because the spectral resolution when ionizing with the second harmonic photons is very good, the nondegenerate 3p levels are partially resolved. According to our previous assignment, the peak at 2.204 eV is due to the $3p_z$ state while the one at 2.251 eV belongs to the symmetry equivalent $3p_x$ and $3p_y$ states. From Figure 5a it is immediately apparent that the two 3p levels follow different dynamics: the $3p_z$ level decays quickly, on a subpicosecond time scale, whereas the $3p_{x,y}$ states linger for several picoseconds.

To model the dynamics we postulate the decay scheme shown in Figure 6. Laser excitation prepares the $3p_z$ and $3p_{x,y}$ Rydberg states with different probabilities, P_z and P_{xy}, arising from the different transition moments from the ground state. The $3p_{x,y}$ states can only decay to 3s in a process that is assumed to be first order with a rate k_2. The $3p_z$ level, which is at higher energy, can decay both into the nearby $3p_{x,y}$ states and the lower lying 3s level. Inspection of Figure 5a shows immediately that the decay of $3p_z$ into the nearby $3p_{x,y}$ states, with a rate k_1, must be much faster than its decay into 3s. The experiment is therefore not very sensitive to the decay $3p_z \rightarrow 3s$, so that we assume its rate to be equal to that of the $3p_{x,y}$ states. This can be reasonably justified because the energy separation between the 3p levels is much smaller than their separation from 3s. The time-dependent decays of the $3p_z$ or $3p_{x,y}$ level, ignoring experimental scaling factors, is thus described as

$$S(3p_z) = P_z \cdot e^{-(k_1+k_2)t} S(3p_{x,y}) = (P_{xy} + P_z \cdot (1 - e^{-k_1 t})) \cdot e^{-k_2 t} \quad (1)$$

At time zero, almost all of the signal arises from $3p_z$, implying that the probability of excitation to $3p_{x,y}$, P_{xy}, is very small. From our data analysis we concluded that $P_z > 0.9$ and $P_{xy} < 0.1$. The computed oscillator strengths for the transitions to those

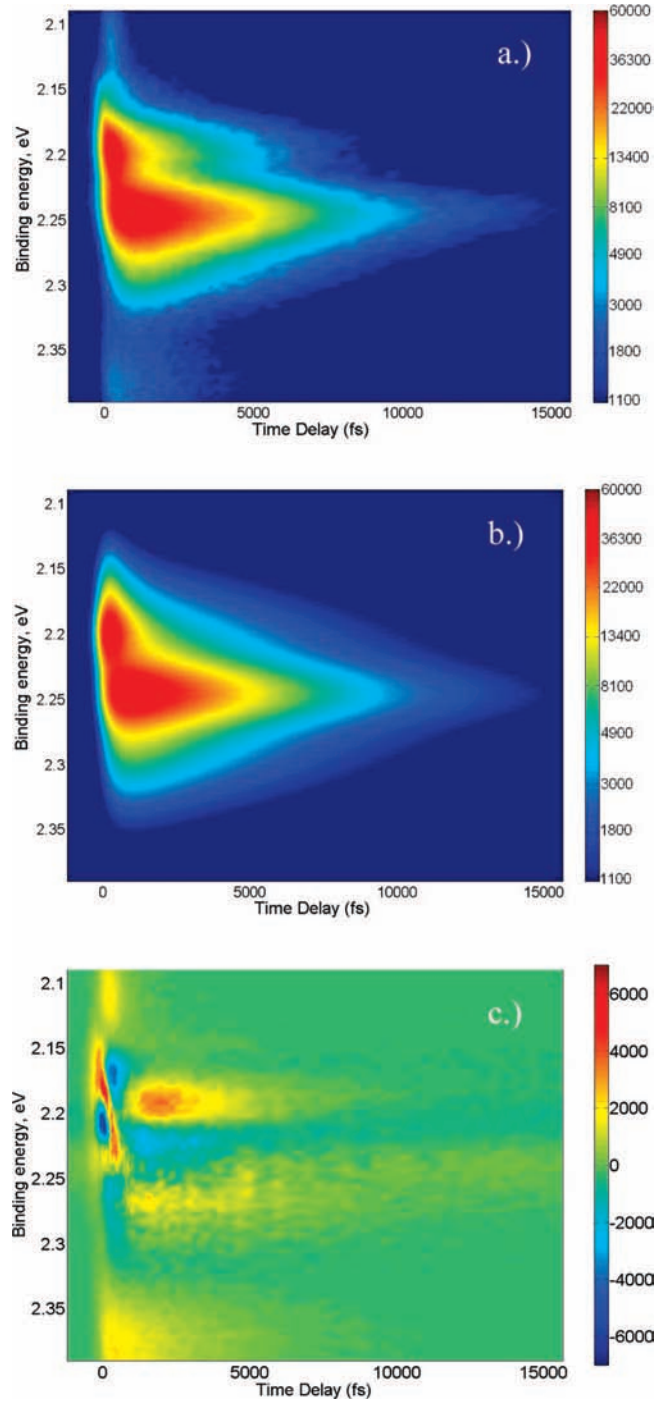

Figure 5. Time-dependent photoionization−photoelectron spectra of TMA upon excitation with one photon at 207.8 nm, observed by ionization with 414 nm. a.) Contour plot of the time-dependent photoelectron spectrum, with the logarithmic intensity given by the color and electron binding energy axis inverted as in Figure 4. b.) Computed fit of the time-dependent spectra using the kinetic electronic relaxation model of Figure 6. c.) The residuals, i.e., the experimental minus the modeled intensities, on a linear color scale. For ease of comparison, all color bars denote the intensities.

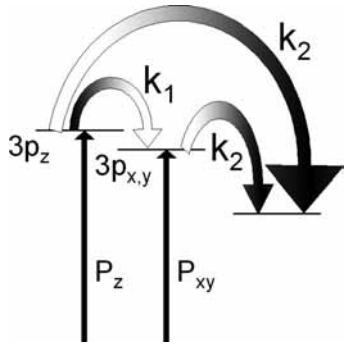

Figure 6. Internal conversion decay pathways used to model the observed decay from the 3p Rydberg states of TMA: the lower $3p_{x,y}$ states decay directly to 3s with a rate of k_2; the higher $3p_z$ state decays both into $3p_{x,y}$ and 3s with rates k_1 and k_2, respectively. P_z and P_{xy} represent the relative excitation probabilities in one-photon excitation to the corresponding 3p Rydberg states from the electronic ground state.

states from the ground state are 0.102 for the nondegenerate transition and 0.0066 for each of the degenerate transitions to $3p_{x,y}$. Thus, while the computed intensity ratio of 8:1 may qualitatively agree with the experimental ratio of larger than 9:1, a quantitative agreement cannot be confirmed. The observation does, however, support our assignment of the 3p levels.

To fit the experimentally measured two-dimensional data, Figure 5a, we assumed that each state ($3p_z$ and $3p_{x,y}$) gives rise to a spectral line that can be represented by the sum of two Gaussians with the same center. The time dependence for each line was modeled as a convolution of the molecular function with the instrument function, which was also assumed to be Gaussian. All parameters, i.e., the time constants and widths of the Gaussians that describe the peak profile, excitation probabilities, and decay rates were optimized simultaneously using the Levenberg−Marquardt algorithm utilizing a unitary weight matrix. Figure 5b shows a delay time/binding energy contour plot calculated using the model and the fit data with the colors again representing the intensities on a natural logarithm scale that displays a large dynamic range.

The two-dimensional fit captures the experimentally observed contour of Figure 5a reasonably well, except for the early time dynamics of the $3p_z$ peak at 2.2 eV. Figure 5c plots the residuals, i.e., the experimental intensity minus the theoretical intensity. The differences are on the order of several thousand intensity units, which is quite small compared to the overall intensity of up to 58 000 units.

The deviation of the observed intensities from those of the model are quite apparent at the early times for binding energies between 2.15 and 2.25. There appear to be oscillations that are not captured by the electronic relaxation model. Since the binding energy decodes the molecular structure, one may be tempted to conclude that we observe oscillatory motions in the molecular structure. Oscillations could, of course, arise from the umbrella motion of the amine group as we excite from the pyramidal ground state to the planar excited state. However, the observed oscillatory period is on the order of 800 fs, which would imply a vibration of 40 cm^{-1}. Since this is an order of magnitude smaller than the frequency of the umbrella motion (about 380 cm^{-1}),[13] it is difficult to see how the umbrella motion could give rise to the observed oscillatory structure. At present we do not understand the origin of the oscillations in the residuals.

Even so, for the $3p_{x,y}$ peak and longer delay times the results of the fit using the stated model are quite satisfactory. The decays of the 3p states are characterized by the following parameters (3σ error bars)

$$k_1 = 1.85 \times 10^{12}\ s^{-1}\ \tau_1 = 540\ \text{fs}(\ 75\text{fs})$$

$$k_2 = 3.47 \times 10^{11}\ s^{-1}\ \ \tau_2 = 2.9\ \text{ps}\ (0.2\ \text{ps}) \quad (2)$$

To complement the photoelectron spectra we also measured the time-dependent mass spectra using the two-photon ionization scheme. Since the probe photon is unable to ionize out of 3s, the time-dependent mass spectrum shows only the decay of the parent ions and only a negligible amount of fragment signal. The decay time mirrors that of the decay of the 3p manifold in the photoelectron spectrum with a rate of k_2.

The marked difference in the decay times of the $3p_z$ and $3p_{x,y}$ states can be understood on the basis of the energy gap law for electronic relaxation processes.[42] For a transition between 'matching' states (i.e., states with potential energy surfaces that do not intersect), the Franck−Condon factors decay exponentially with the energy gap between the involved states because jumps between larger quantum numbers are necessary. The $3p_z$ state has the possibility of decaying into the $3p_{x,y}$ states, which are only 47 meV lower in energy. The closest energy state for the $3p_{x,y}$ states, however, is the 3s level, which is down by 836 meV. This significantly larger energy gap requires a large difference between the vibrational states that take up the released energy, and so the decay time is significantly longer. In this context we note that the transition from $3p_z$ to $3p_{x,y}$ is unusual because of its small change in the electronic energy. It is possible because the molecules already have 0.42 eV of internal energy from the excitation step and the three methyl groups provide a dense bath of low-frequency vibrations that are able to accommodate and match the electronic energy.

4. Conclusions

The study of electronic relaxation phenomena in high-lying electronic states of polyatomic molecules has traditionally been difficult because electronic states are difficult to separate. Overlapping Franck−Condon envelopes and short lifetimes make most absorption and fluorescence spectra impossible to resolve and assign. However, this does not imply that the electronic states and their dynamic energy relaxation pathways are always poorly defined. Indeed, many electronic states do have lifetimes that are sufficiently long lived to allow accurate determination of the electronic relaxation if vibrational congestion is eliminated. To observe such phenomena it is advantageous to use spectroscopic transitions that do not couple with the multitude of vibrational states that are prepared in the initial step or as a result of the electronic energy redistribution. Photoionization from Rydberg states to the ground states of the corresponding ions follows a fairly strict $\Delta v = 0$ selection rule, which enables us to resolve electronic states that were previously buried underneath a broad Franck−Condon envelope.

In trimethylamine, two- and three-photon resonance-enhanced photoionization coupled with photoelectron spectroscopy allows accurate determination of the electron binding energies. The adiabatic ionization energy is obtained as 7.743 eV, and the binding energies of the 3s, $3p_{x,y}$, and $3p_z$ states are 3.087, 2.251, and 2.204 eV, respectively. Depending on the excitation wavelengths, the molecules in those states have significant internal energy, sufficient to cross the barriers to rotation of the methyl groups. All those motions do not affect the spectral resolution, down to the best (14 meV) resolution of our instrument.

Time-resolved experiments allow us to follow the electronic relaxation dynamics of trimethylamine with unprecedented detail. Irradiation at 207.8 nm leads to excitation of the $3p_z$ and $3p_{x,y}$ levels with a > 9:1 ratio. The higher $3p_z$ level decays with

a lifetime of 540 fs to the close lying $3p_{x,y}$ level, which in turn decays on a time scale of 2.9 ps to 3s.

The time-resolved ionization spectra show no evidence for involvement of other electronic states or fragmentation on the 3s surface during the experiment. The appearance energy for fragmentation to the deprotonated species at *m/e* 58 in the ion has been reported as 9.38 eV.[41] With our value for the adiabatic ionization energy of 7.743 eV, this implies that the molecular ion requires more than 1.64 eV to dissociate. With excitation at 207.8 nm the trimethylamine molecule has 0.42 eV of internal energy in 3p, while with excitation at 2 × 400 nm it would have 0.66 eV. Even upon internal conversion to 3s, the molecule's energy, 1.31 eV from 207.8 nm excitation and 1.54 eV from 2 × 400 nm excitation, does not suffice to dissociate, explaining the absence of significant fragmentation. A very small number of fragments could be traced to an alternate ionization pathway in the three-photon experiments, which may deposit sufficient energy for dissociation at the tail end of the Franck−Condon envelope. We note that this situation is in contrast to that found in larger tertiary amines, where the internal conversion from 3p to 3s does deposit sufficient energy for α cleavage.[43] Even so, recent work has shown that the lifetime in 3s is not sufficient to allow the bond to break. Instead, the fragments observed in the mass spectrometer are generated subsequent to ionization on the ion surface.[29]

No electronic states other than the 3s, $3p_{x,y}$, and $3p_z$ states were found in our experiments. If any other states were prepared in the initial photoexcitation, the ionization experiment would most certainly detect it. Our work thus differs from the work by Taylor et al.,[17] who use model calculations to interpret a broadening of the spectral lines observed in 2 + 2 photoionization experiments with mass-selected detection as arising from distinct 3s Rydberg resonances. In analogy to monomethylamine, they suggested that there are states with different charge distributions of the ion cores, which would give rise to either bound or dissociative 3s Rydberg states. No such states need to be invoked to explain any of our experimental or computational results. All the states that we observe are well accounted for by the traditional sequence of Rydberg levels converging to the ground state of the molecular ion.

The time-resolved photoionization experiments described here provide a clear picture of the early time dynamics of the trimethylamine system. The subsequent dynamics includes relaxation to the ground state and the subsequent fragmentation of the hot trimethylamine molecule. Following initial work by Kawasaki et al.,[44] those processes have been thoroughly investigated in a series of recent papers by Butler, Suits, and collaborators.[14,15] Those studies assume that the 3s state is quickly reached regardless of excitation wavelength. The present study supports this point, filling in the time scales and kinetics scheme. Our early-time study and Butler's late-time study intersect where the molecule is on the 3s surface, which we have shown to be reached within 2 ps. The entire photodissociation dynamics of trimethylamine is now well understood.

Acknowledgment. This work was supported by the Division of Chemical Sciences, Geosciences, and Biosciences, the Office of Basic Energy Sciences, the U.S. Department of Energy, by grant no. DE-FG02-03ER15452, and the NIH under grant number 1 R21 HG002961-01A2.

References and Notes

(1) Robin, M. B. *Higher Excited States of Polyatomic Molecules*; Academic Press, Inc.: New York, 1985; Vol. III.

(2) Tannenbaum, E.; Coffin, E. M.; Harrison, A. J. *J. Chem. Phys.* **1953**, *21*, 311.

(3) Walsh, A. D.; Warsop, P. A. *Trans. Faraday Soc.* **1961**, *57*, 345.

(4) Harshbarger, W. R. *J. Chem. Phys.* **1971**, *54*, 2504.

(5) Douglas, A. E. *Discuss. Faraday Soc.* **1963**, *35*, 158.

(6) Douglas, A. E.; Hollas, J. M. *Can. J. Phys.* **1961**, *39*, 479.

(7) Rianda, R.; Frueholz, R. P.; Goddard, W. A., III. *Chem. Phys.* **1977**, *19*, 131.

(8) Runau, R.; Peyerimhoff, S. D.; Buenker, R. J. *J. Mol. Spectrosc.* **1977**, *68*, 253.

(9) Cureton, C. G.; Hara, K.; O'Connor, D. V.; Phillips, D. *Chem. Phys.* **1981**, *63*, 31.

(10) Sato, H.; Kawasaki, M.; Toya, K.; Sato, K.; Kimura, K. *J. Phys. Chem.* **1987**, *91*, 751.

(11) Hager, J.; Ivanco, M.; Wallace, S. *C.; Chem. Phys. Lett.* **1982**, *92*, 112.

(12) Kimura, K.; Katsumata, S.; Achiba, Y.; Yamazaki, T.; Iwata, S. *Handbook of He(I) Photoelectron Spectra of Fundamental Organic Molecules*; Japan Scientific Societies Press: Tokyo, 1981.

(13) Matsumi, Y.; Obi, K. *Chem. Phys.* **1980**, *49*, 87.

(14) Forde, N. R.; Morton, M. L.; Curry, S. L.; Wrenn, S. J.; Butler, L. J. *J. Chem. Phys.* **1999**, *111*, 4558.

(15) Forde, N. R.; Butler, L. J.; Ruscic, B.; Sorkhabi, O.; Qi, F.; Suits, A. *J. Chem. Phys.* **2000**, *113*, 3088.

(16) Halpern, A. M.; Ondrechen, M. J.; Ziegler, L. D. *J. Am. Chem. Soc.* **1986**, *108*, 3907.

(17) Taylor, D. P.; Dion, C. F.; Bernstein, E. R. *J. Chem. Phys.* **1997**, *106*, 3512.

(18) Minitti, M. P.; Cardoza, J. D.; Weber, P. M. *J. Phys. Chem. A* **2006**, *110*, 10212.

(19) Minitti, M. P.; Weber, P. M. *Phys. Rev. Lett.* **2007**, *98*, 253004.

(20) Cardoza, J. D.; Weber, P. M. *J. Chem. Phys.* **2007**, *127*, 036101.

(21) Kuthirummal, N.; Weber, P. M. *J. Mol. Struct.* **2006**, *787*, 163.

(22) Cheng, W.; Kuthirummal, N.; Gosselin, J.; Sølling, T. I.; Weinkauf, R.; Weber, P. M. *J. Phys. Chem. A* **1920**, *109*, 2005.

(23) Kuthirummal, N.; Weber, P. M. In *Femtochemistry and Femtobiology: Ultrafast Events in Molecular Science*; Martin M.; Hynes J. T., Eds.; Elsevier: New York, 2004; p 37.

(24) Achiba, Y.; Sato, K.; Shobatake, K.; Kimura, K. *J. Chem. Phys.* **1983**, *78*, 5474.

(25) Glownia, J. H.; Riley, S. J.; Colson, S. D.; Miller, J. C.; Compton, R. N. *J. Chem. Phys.* **1982**, *77*, 68.

(26) Schick, C. P.; Weber, P. M. *J. Phys. Chem. A* **2001**, *105*, 3735–3740.

(27) Kuthirummal, N.; Weber, P. M. *Chem. Phys. Lett.* **2003**, *378*, 647–653.

(28) Gosselin, J. L.; Weber, P. M. *J. Phys. Chem. A* **2005**, *109*, 4899.

(29) Gosselin, J. L.; Minitti, M. P.; Rudakov, F. M.; Sølling, T. I.; Weber, P. M. *J. Phys. Chem. A* **2006**, *110*, 4251.

(30) Minitti, M. P.; Gosselin, J. L.; Sølling, T. I.; Weber, P. M. *FemtoChemistry VII*; Castleman, A. W.; Jr.; Kimble, M. L., Eds.; Elsevier: New York, 2006; pp 44−48.

(31) Conaway, W. E.; Morrison, R. J. S.; Zare, R. N. *Chem. Phys. Lett.* **1985**, *113*, 429.

(32) Kim, B.; Thantu, N.; Weber, P. M. *J. Chem. Phys.* **1992**, *97*, 5384.

(33) Schick, C. P.; Carpenter, S. D.; Weber, P. M. *J. Phys. Chem. A* **1999**, *103*, 10470.

(34) Aue, D. H.; Webb, H. M.; Bowers, M. T. *J. Am. Chem. Soc.* **1976**, *98*, 311.

(35) Halpern, A. M.; Gerrity, D. J.; Rothman, L. J.; Vaida, V. *J. Phys. Chem.* **1982**, *76*, 102.

(36) Parker, D. H.; Bernstein, R. B.; Lichtin, D. A. *J. Phys. Chem.* **1981**, *75*, 2577.

(37) Avouris, P.; Rossi, A. R. *J. Phys. Chem.* **1981**, *85*, 2340.

(38) Lide, D.; Mann, D. E. *J. Chem. Phys.* **1958**, *28*, 572.

(39) The normal mode frequencies obtained in our DFT calculation are as follows, in cm^{-1}: 248, 260*, 346, 427*, 841, 1071*, 1084, 1134*, 1223, 1322*, 1467*, 1508*, 1510, 1520, 1531, 1540*, 2920*, 2937, 3072*, 3077, 3115, 3120*; the asterisks indicate degenerate vibrations.

(40) Durig, J. R.; Craven, S. M.; Bragin, J. *J. Chem. Phys.* **1970**, *53*, 38.

(41) Lossing, F. P.; Lam, Y.-T.; Maccoll, A. *Can. J. Chem.* **1981**, *59*, 2228.

(42) Turro, N. J. *Modern Molecular Photochemistry*; University Press: Menlo Park, 1978; p 172.

(43) Sölling, T. I.; Kötting, C.; Zewail, A. H. *J. Phys. Chem. A* **2003**, *107*, 10872.

(44) Kawasaki, M.; Kasatani, K.; Sato, H.; Shinohara, H.; Nishi, N.; Ibuki, T. *J. Chem. Phys.* **1982**, *77*, 258.

JP8041236